Available online at www.eccomasproceedia.org
Eccomas Proceedia SMART (2023) 226-237

ECCOMAS
Proceedia

X ECCOMAS Thematic Conference on Smart Structures and Materials
SMART 2023
D.A. Saravanos, A. Benjeddou, N. Chrysochoidis and T. Theodosiou (Eds)

EFFECT OF A RESONANT PIEZOELECTRIC SHUNT ON THE STRUCTURAL VIBRATIONS OF A TRUNCATED HYDROFOIL

Y. Watine*, B. Lossouarn†, C. Gabillet*, J.-F. Deü†, J.-A. Astolfi*

*Institut de Recherche de l'Ecole Navale (IRENav),
EA 3634 - Ecole Navale, 29240, Brest, France.

† Laboratoire de Mécanique des Structures et des Systèmes Couplés (LMSSC),
Conservatoire national des arts et métiers (Cnam),
292 rue Saint-Martin, 75003, Paris, France. HESAM Université.

Abstract. Immersed marine structures such as hydrofoils or propeller blades may undergo severe flow induced vibrations when a hydrodynamic excitation source couples with a natural frequency of the structure. This phenomenon, known as lock-in, induces acoustic radiations and structural fatigue. High amplitude vibrations will also impact the near-wake region leading to a modification of the vortex dynamics. The present study consists of a numerical and experimental investigation of the impact of a resonant piezoelectric shunt on the structural vibrations of a truncated hydrofoil. The system consists of a MFC piezoelectric patch integrated in a NACA 66-306 profile and connected to a ferrite core inductor. A finite element model was created using the software COMSOL Multiphysics in order to predict the electro-mechanical properties of the system. Experimental tests are then realized at zero degrees of incidence in the hydrodynamic tunnel of the French Naval Academy Research Institute at zero flow velocity and at 4.4 $\mathrm{m.s^{-1}}$. The mechanical response of the hydrofoil is investigated using laser vibrometry. The electrical resonance of the shunt is tuned to reduce the vibrations induced by the lock-in with the twisting mode occurring at a flow velocity of 4.4 $\mathrm{m.s^{-1}}$. A vibration reduction of 59 % is observed for this particular set-up. The passive resonant piezoelectric shunt is an efficient, simple and cost-effective technique to reduce flow induced vibrations. It will pave the way for various smart structure applications.

Key words: vibration mitigation, vortex shedding, piezoelectric coupling, resonant shunt

1 INTRODUCTION

Solid bodies, when placed in a steady flow at high Reynold number, induce hydrodynamic instabilities which are responsible for periodic and alternative vortex shedding which acts as a structural excitation source and induces body vibrations [1, 2]. When the vortex shedding frequency coincides with a natural frequency of the structure, a drastic increase of the vibration

Peer-review under responsibility of the organizing committee of SMART 2023.
doi: 10.7712/150123.9780.444936

magnitude occurs [3]. This phenomenon, known as lock-in, may have dramatic consequences for various industrial applications.

Nowadays, lifting surfaces are used extensively in the marine engineering domain and are particularly prone to Flow Induced Vibrations (FIV). For example, hydrofoils are used on fast sailing yachts [4] navigating at velocities where vibrations induce major concerns in terms of structural fatigue. In the naval domain, the design of rotative machinery including ship propeller blades and centrifugal pumps requires special attention in order to reduce as much as possible the flow induced vibrations to avoid acoustic radiation. Hydraulic machinery consisting of turbines and pumps containing stay and guide vanes are also strongly impacted by FIV [5].

Over the years numerous research projects have investigated, both experimentally and numerically, the mechanism leading to FIV in order to understand its principle and find solutions to reduce the vibrations, see [6, 7]. Commonly adopted vibration mitigation methods consist in the modification of existing structures by suppression or addition of material. For example, the modification of a hydrofoil trailing edge is able to drastically reduce the vibration magnitude and the range of flow velocities where coupling occurs [8]. However, these solutions may also minimize the performance of the lifting surface. More advanced systems such as wake control by acoustic waves generation [9] or boundary layer blowing and suction [10], have also been investigated but require the integration of complex systems often not adapted for marine devices. Regarding the high requirement level proper to modern marine applications, it is necessary to develop vibration mitigation devices which are highly adaptative, robust and easy to integrate on various types of structures.

Piezoelectricity is the ability of certain materials to generate an electric field when a mechanical force is applied to it and reversely to generate a deformation if it is exposed to an electric field. Some transducers based on piezocomposites consist of thin patches which are deformable and robust due to an encapsulating protective shell. These properties enable easy integration on various complex structures such as propeller blades or hydrofoils. Vibration mitigation can be achieved when a piezoelectric transducer is connected to an inductor and a resistor. This simple electrical circuit is named a passive resonant shunt and is based on the tuning of an electrical resonance frequency with a mechanical frequency to reach optimal vibration mitigation [11]. Only few tests have been conducted to mitigate vibrations in water [12], especially for twisting type vibrations. Gaining new insight in this configuration will permit to use resonant piezoelectric shunts to mitigate vibrations of marine lifting surfaces.

The present work aims to describe the effect of a passive resonant piezoelectric shunt on the vortex induced vibrations sustained by a NACA 66-306 truncated hydrofoil at high Reynolds number. After presenting the experimental set-up, a numerical model of the hydrofoil embedded with DuraAct and MFC type transducers is assessed. The aim of this model is to predict accurately the natural frequencies and coupling factors of a structure embedded with piezoelectric transducers in order to facilitate future designs of prototypes. Then, the vibration mitigation induced by the resonant shunt at zero flow velocity and at the flow velocity where the lock-in occurs is investigated experimentally.

2 EXPERIMENTAL ARRANGEMENT

2.1 Hydrodynamic tunnel

The hydrodynamic tunnel of the French Naval Academy Research Institute (IRENav) enables to study two- or three-dimensional fluid flows around obstacles with an average size of 100 mm. The test section, which is the part where the studied profiles are located, is 192 mm squared and 1 m long. The turbulence intensity at the entrance of the test section is 2%. A programmable logic controller is used for monitoring and regulation of the flow velocity in the tunnel. The upstream velocity and pressure at the entrance of the test section are regulated with a relative accuracy of ±2% and ±2.5% respectively. For the present study, the flow velocity was varied from 3.0 to 5.5 $\mathrm{m.s}^{-1}$ which corresponds to a Reynolds number range $[2.55 \times 10^5; 4.68 \times 10^5]$.

2.2 Truncated hydrofoil structure

The studied geometry consists of a NACA 66-306 aluminium hydrofoil with a maximum thickness of 6% at 45.46% of the chord. The hydrofoil had an original chord of 100 mm but was truncated at 85% of the original chord. The final dimensions are 191.0 mm × 85.0 mm × 6.13 mm (span s, chord c, thickness D). The root of the foil has been specially manufactured to form a cantilevered structure with a perfect clamping condition at the backside of the test section. The hydrofoil is mounted in the test section with zero incidence, assuming that the uncertainty in the angle of attack is 0.1°. See figure 1 for an illustration of the hydrofoil.

On the suction side of the hydrofoil, a rectangular cavity of dimension 108 mm × 68 mm × 0.5 mm was machined to host a MFC piezoelectric patch of the type $M8557F1$. The remaining space between the cavity and the patch has been filled with epoxy in order to maintain the patch. The MFC patch is primarily designed to sustain twisting type actuation and sensing due to the direction of the composite piezoelectric fibres equal to 45 °. The MFC patch is connected to an electrical shunt circuit and can be used for structural vibration mitigation. On the pressure side of the hydrofoil, another rectangular cavity of dimension 61.5 mm × 71 mm × 1 mm has been

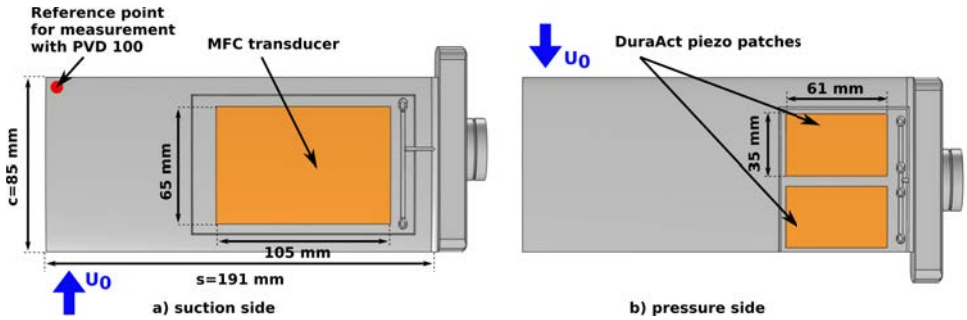

Figure 1: Truncated NACA 66-306 hydrofoil geometry and piezoelectric patch arrangement. Views of the suction and pressure side. U_0 indicates the direction of the free-stream flow.

	Deflection shape	
First mode frequency in air f_1^{air}	92.5 Hz	Bending
First mode frequency in water f_1^{water}	39.4 Hz	
Second mode frequency in air f_2^{air}	518.4 Hz	Torsion
Second mode frequency in water f_2^{water}	281.2 Hz	
Third mode frequency in air f_3^{air}	637.2 Hz	Bending
Third mode frequency in water f_3^{water}	302.8 Hz	

Table 1: Natural frequencies and types of modes of the hydrofoil immersed in air and in water.

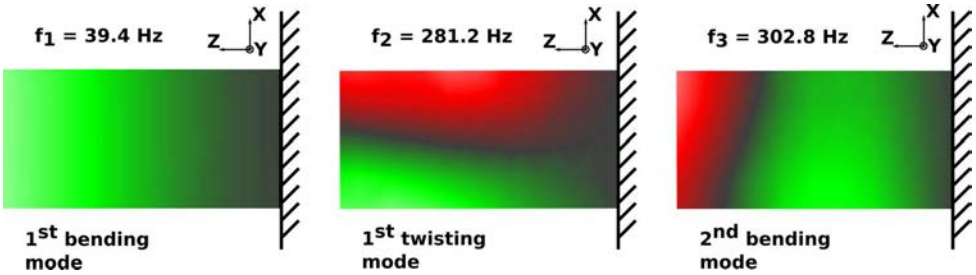

Figure 2: Experimental deflection shapes associated with the first three natural frequencies for the hydrofoil immersed in water.

machined in order to insert two P-876.A15 DuraAct patches. This second cavity is aligned on the trailing edge in order to force a twisting type deformation when the DuraAct patches are supplied by voltage and used as a structural excitation source.

Laser vibrometry is a contactless vibration measurement method using the Doppler effect principle. The phase shift between the emitted and received laser signals provides characterization of the displacement velocity related to the structure. Mode shapes and natural frequencies were characterized in still air and in still water. The results are summarized in table 1. This was made by analysing the vibration response of the structure at a reference point to a white noise signal of bandwidth 0 to 2 kHz supplied to the two DuraAct piezoelectric transducers. The modes shapes associated with each natural frequency when the hydrofoil is surrounded by water are presented by figures 2.

2.3 Passive resonant piezoelectric shunt principle

A series resonant piezoelectric shunt is composed of a piezoelectric transducer of capacitance C connected to a resistance R_t and an inductor L_{eq}. The piezoelectric effect of the patch is exploited to convert mechanical energy into electrical energy which is then dissipated through the resistance by Joule effect. The inductor introduces an electrical resonance which has the specificity of increasing the electrical current flowing through the resistance and thereby maximises the dissipation. The electrical resonance of the circuit is usually tuned to a mechanical natural

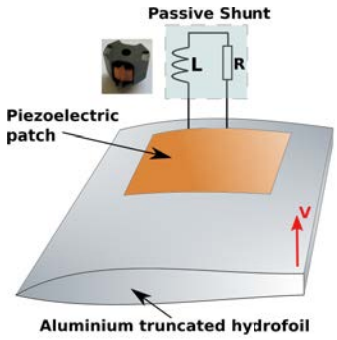

Figure 3: Passive resonant piezoelectric shunt principle. V corresponds to the displacement velocity.

frequency of the structure in order to mitigate a mechanical resonance [12]. Figure 3 presents the general arrangement of a passive resonant piezoelectric shunt paired with a hydrofoil type structure. The efficiency of the shunt to reduce the vibrations depends on the coupling factor k_c which is expressed as

$$k_c = \sqrt{\frac{\omega_{oc}^2 - \omega_{sc}^2}{\omega_{sc}^2}}, \tag{1}$$

where ω_{oc} corresponds to the natural angular frequency of the foil structure when the piezoelectric transducer is in open-circuit and ω_{sc} is the natural angular frequency of the structure when the piezoelectric patch is in short-circuit. For relatively low piezoelectric coupling factors, the optimal values of R_t and L_{eq} are [11]:

$$L_{eq} = \frac{1}{C\omega_{oc}^2}, \tag{2}$$

$$R_t = \sqrt{\frac{3}{2}}\frac{k_c}{C\omega_{oc}}. \tag{3}$$

For the present study a simple coper wired inductance with a ferrite core was used. This type of inductor is designed for the high voltage measured at the output of the MFC transducer when the vibration level is high. The resonant shunt described here does not require an external source of energy which makes it particularly adapted for marine applications.

3 NUMERICAL COMPUTATIONS

3.1 Purpose

The use of a numerical tool to predict the modal properties and the coupling factors of structures embedded with piezoelectric transducers is of great interest because it will avoid several, time consuming and expensive, experimental iterations. The commercial code COMSOL *Multiphysics*, based on finite elements computations, was employed to implement a numerical model

of the hydrofoil embedded with piezoelectric transducers. The modelling of a MFC transducer is still challenging and we present here a calibration method of its piezoelectric constants which could be employed for the design of other structures embedded with MFC piezocomposites. After describing the setup of the numerical model, the present section describes the computed modal properties and coupling factors.

3.2 Modelling of the fluid and hydrofoil structure

A CAD file including the hydrofoil structure, the piezoelectric active layers, the Kapton shells and the epoxy was first generated. For simplicity, Kapton and Epoxy were considered as the same material, identified here as "soft layer" [12]. A fixed constraint condition was applied at the root of the hydrofoil in order to model a perfect clamping, see figure 4a for an illustration. This element is important because the clamping conditions may affect the mode shapes and thus the coupling factor.

The numerical study in still water requires an additional domain representative of the test section and the fluid. A parallelepiped bloc of same dimensions as the test section was implemented with the hydrofoil located at the center of the lateral wall, as displayed in figure 4b. The fluid domain, which consists of an acoustic fluid medium surrounding the hydrofoil, is representative of the water present in the test section. Rigid walls boundary conditions were applied to the lateral faces of the fluid domain. This type of boundary implies that the acoustic radiation, is restricted by the walls. The input and the output of the fluid domain represents the locations where the flow enters the test section and where it goes out. These surfaces have been configured in order that the acoustic pressure vanishes at these locations. The fluid was considered at rest (zero flow velocity) for all the computations.

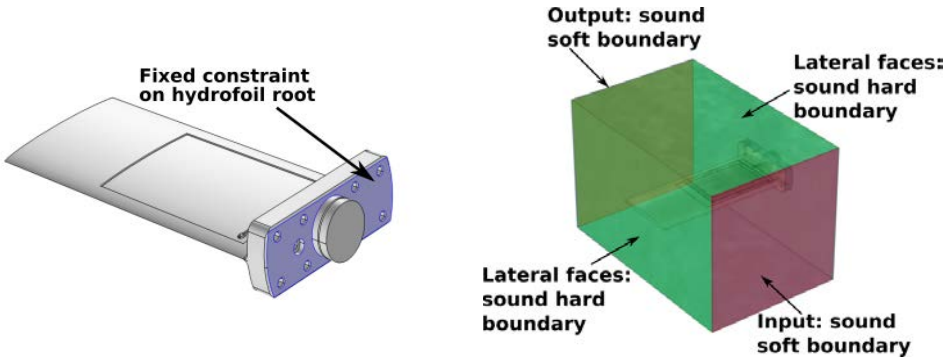

(a) (b)

Figure 4: (a) Hydrofoil geometry with a fixed constraint applied at the root of the profile. (b) fluid domain surrounding the hydrofoil for numerical computation in still water.

3.3 Modelling of a MFC transducer

3.3.1 Mixing rules

Macro Fiber Composites (MFCs) have been developed at NASA around the year 2000 [13]. They consist of rectangular piezo-ceramic fibres sandwiched between layers of adhesive, electrodes and polyamide film. The MFC transducer used for this study is a $M8557F1$ manufactured by *Smart Material*. This type of transducer is composed of several layers of different materials (electrodes, kapton, epoxy, active layer) which means that an accurate numerical modelling is not straightforward. A detailed description of the layer sequence, thickness and equivalent homogenous mechanical, piezoelectric and dielectric properties of each constitutive material is required to obtain realistic simulations. These technical data are in general not provided by the manufacturers. The present study proposes to use the homogenized properties derived from analytical mixing rules proposed by [14] combined with a calibration of the piezoelectric and permittivity parameters in order to match with the experimental coupling factors and the capacitance. The homogenized properties of the d_{33} MFC active layer are summarized in table 2.

The homogenized compliance matrix for the d_{33} MFC transducer is considered as a transversely isotropic material which is a special form of orthotropic material [15]. The compliance

d_{33} **MFC homogenized properties**	**Symbol**	**Unit**	**Mixing rules**
Young's modulus	E_1	GPa	16.97
	E_2	GPa	42.18
Shear modulus	G_{12}	GPa	6.06
	G_{23}	GPa	17
Poisson's ratio	ν_{21}	-	0.38
	ν_{23}	-	0.24
Piezoelectric charge constants	d_{32}	pC/N	-176
	d_{33}	pC/N	436
Dielectric relative constant (free)	$\epsilon_{33}^T/\epsilon_0$	-	1593

Table 2: Homogenized properties of the active layer of a d_{33} MFC calculated by [14] using analytical mixing rules.

matrix is expressed as

$$[S] = \begin{bmatrix} \frac{1}{E_1} & -\frac{\nu_{21}}{E_2} & -\frac{\nu_{21}}{E_2} & 0 & 0 & 0 \\ -\frac{\nu_{21}}{E_2} & \frac{1}{E_2} & -\frac{\nu_{23}}{E_2} & 0 & 0 & 0 \\ -\frac{\nu_{21}}{E_2} & -\frac{\nu_{23}}{E_2} & \frac{1}{E_2} & 0 & 0 & 0 \\ 0 & 0 & 0 & \frac{1}{G_{23}} & 0 & 0 \\ 0 & 0 & 0 & 0 & \frac{1}{G_{12}} & 0 \\ 0 & 0 & 0 & 0 & 0 & \frac{1}{G_{12}} \end{bmatrix}, \tag{4}$$

where the direction 1 corresponds to the in-plane orthogonal to the fibres direction, 2 the normal out-of-plane direction and 3 the fibres direction. Transverse isotropy induces that $\nu_{12}/E_1 = \nu_{21}/E_2$. Note that it is direction 1 that offers different properties (and not the direction of the fibers) because a 3D representation of this equivalent material would actually be a stack of piezoelectric layers normal to direction 1.

3.3.2 Calibration of the piezoelectric properties

The experimental MFC patch is of type d_{33} but in order to avoid the modelling of the inter-digitated electrodes, a d_{31} equivalent model is implemented. A calibration of this model was done by multiplying the relative permittivity parameters proposed in [14] by a constant value. The piezoelectric charge constants of the active layer (d_{21}, d_{22}, d_{23}) were then adjusted to match the experimental coupling factors of the in-air configuration. The modified charge constants and permittivities were not modified for the in-water configuration and were kept the same for all the upcoming computations.

3.4 Computation of the natural frequencies and deflection shapes

The natural frequencies and associated deflection shapes were computed for the in water configuration with all the transducers in open-circuit. This type of analysis offers substantial informations about the deformation of the structure and may help to identify critical stress regions and critical vibration regimes. Figure 5 presents the deflection shapes of the first three natural modes and their associated natural frequencies. The highest deformation magnitude is represented by dark blue regions and lowest by light green regions. The transparent frame represents the structure without deflection. The first mode is a bending mode, the second mode is a twisting mode and the third mode is close to a second bending mode but the non-symmetric geometry leads to a combination of bending and twisting deformation. These deflection shapes are in agreement with the ones observed with the scanning vibrometer (figure 2).

The experimental and numerical natural frequencies are presented in table 3. For the first three modes, the difference between experimental and numerical values is lower than 3% without recalibration of the mechanical properties. These results demonstrate the benefits of preliminary numerical computations. Especially, knowing the natural frequencies at the early design stage will prevent post-manufacturing modifications of the structure.

	Open-circuit, numerical	Open-circuit, experimental	error
f_1	38.43 Hz	39.38 Hz	2.4%
f_2	285.54 Hz	281.2 Hz	1.5%
f_3	302.28 Hz	302.8 Hz	0.2%

Table 3: Numerical and experimental frequencies of the first three modes in water with MFC electrodes in open-circuit

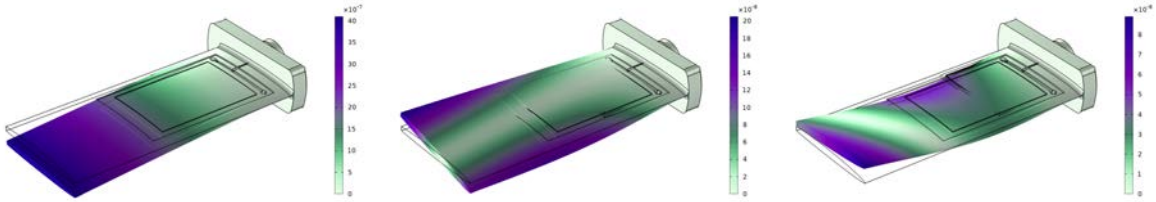

(a) Mode 1: $f_1 = 38.43\ Hz$ (b) Mode 2: $f_2 = 285.54\ Hz$ (c) Mode 3: $f_3 = 302.28\ Hz$

Figure 5: Mode shapes of the hydrofoil structure obtained by numerical simulation with COMSOL *Multiphysics*. The hydrofoil is immersed in water.

3.5 Computation of the Piezoelectric coupling factors

The capability of a resonant piezoelectric shunt to mitigate vibrations is directly dependent of the coupling factors. The coupling factor relies on the piezoelectric material properties but also on the positioning of the transducer on the structure and on the soft layer features.

A comparison between numerical and experimental results is presented in table 4. As stated before, the piezoelectric constants of the MFC patch were calibrated in air so that the experimental and numerical coupling factors of the second bending mode (kc_2) match together. After calibration, it appears that the coupling factors proper to modes one (kc_1) and three (kc_3) are also aligned. Results for the in water configuration reveal also a proper match of the numerical and experimental coupling factors.

4 EXPERIMENTAL RESULTS

4.1 Vibration mitigation at zero flow velocity

A passive resonant piezoelectric shunt was implemented with a copper wired inductor and tested with the hydrofoil immersed in water at zero flow velocity. The structure was excited by using the two DuraAct patches connected to a signal generator and a power amplifier. The reader can refer to table 5 for a complete overview of the shunt parameters. As displayed in figure 6a showing the frequency response functions in short-circuit, open-circuit and with the shunt activated, an attenuation level of 17 dB of the first twisting mode was reached. Ideal tuning of the shunt should provide an off-peak centred on the natural frequency to attenuate.

Air			**Water**		
f_n^{num}	kc_n^{num}	kc_n^{exp}	f_n^{num}	kc_n^{num}	kc_n^{exp}
$f_1^{sc} = 87.68\ Hz$	3.04%	3.3%	$f_1^{sc} = 38.416\ Hz$	3.10%	3.70%
$f_1^{oc} = 87.72\ Hz$			$f_1^{oc} = 38.434\ Hz$		
$f_2^{sc} = 517.41\ Hz$	9.15%	9.2%	$f_2^{sc} = 284.58\ Hz$	8.20%	8.50%
$f_2^{oc} = 519.57\ Hz$			$f_2^{oc} = 285.54\ Hz$		
$f_3^{sc} = 629.57\ Hz$	2.61%	2.7%	$f_3^{sc} = 301.91\ Hz$	4.95%	4.70%
$f_3^{oc} = 629.71\ Hz$			$f_3^{oc} = 302.28\ Hz$		

Table 4: Coupling factors proper to the MFC transducer.

Experimental shunt parameters	
Coupling factor	8.47%
Inductance	20.4 H (100 Hz) and 21.46 H (1 kHz)
Equivalent series resistance (iron and copper)	618 Ω (100 Hz) and 750 Ω (1 kHz)

Table 5: Parameters of the copper wired inductor shunt used for optimal vibration mitigation with the hydrofoil surrounded by water at zero flow velocity. Inductance and resistance were recorded a two different frequencies (100 Hz and 1 kHz).

However, it is rather a broadband peak with a "plateau" centred on f_2 that is observed here. This specificity is due to the fact that the electrical circuit is slightly too resistive, probably because of the internal dissipation of the MFC patch.

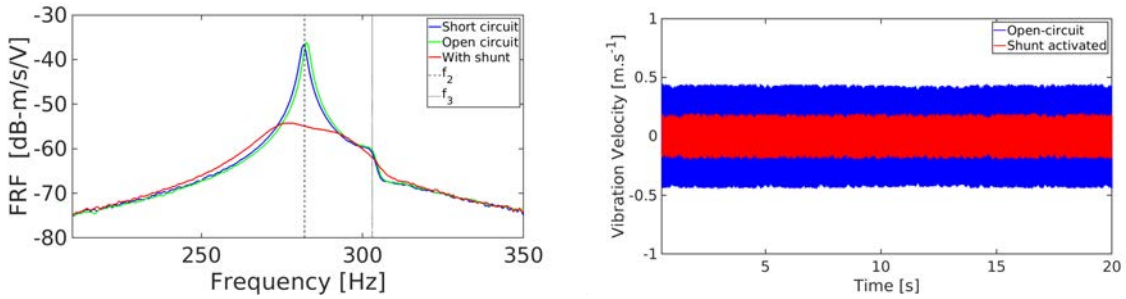

(a) (b)

Figure 6: (a) Frequency response function with the piezoelectric transducer in short-circuit, open circuit and with the copper wired inductor shunt at zero flow velocity in water. A vibration mitigation of 17 dB is observed. (b) Vibration velocity time signal at $\mathrm{U}_0 = 4.4\ \mathrm{m.s}^{-1}$ (lock-in regime) in open circuit and with shunt.

4.2 Vibration mitigation at lock-in

The vibration mitigation level induced by the resonant passive shunt connected to the MFC transducer was investigated at the lock-in regime by comparing the vibration velocity signal root mean square value V_s^{rms} when the shunt is activated and when it is not. It appeared that the optimal value after manual calibration L_{eq}=12 H, is much lower than the one used for the zero flow velocity test. This is probably due to the fact that the MFC patch suffers from water infiltration which induces an increase of the patch capacitance and high internal dissipation. Figure 6b presents the vibration velocity signal at $Re_c = 3.74 \times 10^5$ corresponding to the lock-in with the first twisting mode (f_2). It appears that V_s^{rms} is reduced by 59% which offers a considerable reduction of structural fatigue and acoustic radiation.

5 CONCLUSIONS

A numerical model of a truncated NACA 66-306 hydrofoil embedded with a MFC and with two DuraAct piezoelectric transducers was assessed with the finite element software COMSOL *Multiphysics*. The computations allowed to accurately predict the natural frequencies and deflection shapes of the structure as well as the piezoelectric recalibrated coupling factors of the three first modes. The numerical model described here offers an effective and low-cost tool for designing structures embedded with piezoelectric transducers. The passive resonant shunt was tested experimentally with the hydrofoil surrounded by water at zero flow velocity. In this configuration a significant vibration mitigation level of 17 dB was observed. The shunt was then tested at a flow velocities $U_0 = 4.4\ \mathrm{m.s^{-1}}$ corresponding to the lock-in with the first twisting mode f_2 and provided a reduction of the vibration velocity signal root mean square value V_s^{rms} of 59%. Tests of a passive resonant shunt used to mitigate a twisting mode vibration in a water flow had, to our best knowledge, not been investigated before and the results presented here will pave the way to various industrial applications in the naval domain aiming at reducing flow induced vibrations. We believe that higher vibration mitigation levels could be reached if a better insight on the internal resistance of the piezoelectric transducer is obtained and if water infiltration inside the MFC patch is avoided.

REFERENCES

[1] S. K. Chakrabarti, *The theory and practice of hydrodynamics and vibration*. World scientific, 2002, vol. 20.

[2] E. Naudascher and D. Rockwell, *Flow-induced vibrations: an engineering guide*. Courier Corporation, 2012.

[3] Y. Watine, C. Gabillet, B. Lossouarn, J.-F. Deü, and J.-A. Astolfi, "Vortex-induced vibrations of a cantilevered blunt plate: Pod of tr-piv measurements and structural modal analysis," *Journal of Fluids and Structures*, vol. 117, p. 103832, 2023.

[4] V. Temtching Temou, O. Fagherazzi, B. Augier, J.-A. Astolfi, and D. Raison, "An ex-

perimental and numerical study of fsi applied to sail yacht flexible hydrofoil with large deformations," in *FIV2018-9th International Symposium on fluid-structure interactions, Flow-Sound interactions, flow-induced vibration & noise. July 8-11, 2018, Toronto, Ontario, Canada*, 2018.

[5] A. Zobeiri, "Effect of hydrofoil trailing edge geometry on the wake dynamics," Ph.D. dissertation, École Polytechnique Fédérale de Lausanne, 2012.

[6] W. K. Blake, "Excitation of plates and hydrofoils by trailing edge flows," *Journal of Vibration, Acoustics, Stress, and Reliability in Design*, vol. 106, no. 3, pp. 351–363, 07 1984.

[7] A. Leonard and A. Roshko, "Aspects of flow-induced vibration," *Journal of Fluids and Structures*, vol. 15, no. 3-4, pp. 415–425, 2001.

[8] A. Zobeiri, P. Ausoni, F. o. Avellan, and M. Farhat, "Experimental investigation of the vortex shedding in the wake of oblique and blunt trailing edge hydrofoils using piv-pod method," in *Fluids Engineering Division Summer Meeting*, vol. 54518, 2010, pp. 149–154.

[9] K. Roussopoulos, "Feedback control of vortex shedding at low reynolds numbers," *Journal of Fluid Mechanics*, vol. 248, pp. 267–296, 1993.

[10] D. Park, D. Ladd, and E. Hendricks, "Feedback control of von kármán vortex shedding behind a circular cylinder at low reynolds numbers," *Physics of fluids*, vol. 6, no. 7, pp. 2390–2405, 1994.

[11] O. Thomas, J. Ducarne, and J.-F. Deü, "Performance of piezoelectric shunts for vibration reduction," *Smart Materials and Structures*, vol. 21, no. 1, p. 015008, 2011.

[12] L. Pernod, B. Lossouarn, J.-A. Astolfi, and J.-F. Deü, "Vibration damping of marine lifting surfaces with resonant piezoelectric shunts," *Journal of Sound and Vibration*, vol. 496, p. 115921, Mar. 2021.

[13] W. K. Wilkie, R. G. Bryant, J. W. High, R. L. Fox, R. F. Hellbaum, A. Jalink Jr, B. D. Little, and P. H. Mirick, "Low-cost piezocomposite actuator for structural control applications," in *Smart structures and materials 2000: industrial and commercial applications of smart structures technologies*, vol. 3991. SPIE, 2000, pp. 323–334.

[14] A. Deraemaeker, H. Nasser, A. Benjeddou, and A. Preumont, "Mixing rules for the piezoelectric properties of macro fiber composites," *Journal of intelligent material systems and structures*, vol. 20, no. 12, pp. 1475–1482, 2009.

[15] M. W. Hyer and S. R. White, *Stress analysis of fiber-reinforced composite materials*. DEStech Publications, Inc, 2009.